

This item was submitted to Loughborough's Institutional Repository (<https://dspace.lboro.ac.uk/>) by the author and is made available under the following Creative Commons Licence conditions.



**CC creative commons**  
COMMONS DEED

**Attribution-NonCommercial-NoDerivs 2.5**

**You are free:**

- to copy, distribute, display, and perform the work

**Under the following conditions:**

**BY:** **Attribution.** You must attribute the work in the manner specified by the author or licensor.

**Noncommercial.** You may not use this work for commercial purposes.

**No Derivative Works.** You may not alter, transform, or build upon this work.

- For any reuse or distribution, you must make clear to others the license terms of this work.
- Any of these conditions can be waived if you get permission from the copyright holder.

**Your fair use and other rights are in no way affected by the above.**

This is a human-readable summary of the [Legal Code \(the full license\)](#).

[Disclaimer](#) 

For the full text of this licence, please go to:  
<http://creativecommons.org/licenses/by-nc-nd/2.5/>

# **AN EXPERIMENTAL STUDY OF THE DUAL FUEL PERFORMANCE OF A SMALL COMPRESSION IGNITION DIESEL ENGINE OPERATING WITH THREE GASEOUS FUELS**

**J Stewart<sup>1</sup>, A Clarke<sup>2#</sup> and R Chen<sup>1</sup>**

Department of Aeronautical and Automotive Engineering<sup>1</sup>,

Wolfson School of Mechanical and Manufacturing Engineering<sup>2</sup>,

Loughborough University, UK.

# Corresponding Author a.clarke@lboro.ac.uk

## **ABSTRACT**

A dual fuel engine is a compression ignition (CI) engine where the primary gaseous fuel source is pre-mixed with air as it enters the combustion chamber. This homogenous mixture is ignited by a small quantity of diesel; the 'pilot'; that is injected towards the end of the compression stroke. In the present study, a direct injection CI engine, was fuelled with three different gaseous fuels; methane, propane and butane. The engine performance at various gaseous concentrations were recorded at 1500rpm and  $\frac{1}{4}$ ,  $\frac{1}{2}$ , and  $\frac{3}{4}$  load relative to full load of 18.7kW. In order to investigate the combustion performance, a three zone heat release rate analysis was applied to the data. The resulting mass burned rate data are used to aid understanding of the performance characteristics of the engine in dual fuel mode.

Data are presented for the brake specific energy consumption of the engine and combustion phasing. The highest primary fuel substitution levels were achieved when

using methane under all test conditions and butane proved to be the most unsatisfactory of the three primary fuels. The most promising fuel was found to be propane.

Key Words: Dual fuel, alternative fuels, heat release analysis and combustion phasing.

## **1.0 INTRODUCTION**

The term “dual fuel” refers to a CI engine where a homogenous mixture of gaseous fuel and air is ingested. The ignition source is the injection of a small quantity of diesel fuel, and the overall combustion process is similar to that of a diesel engine. The objective of this technique is to reduce problematic diesel engine emissions of NO<sub>x</sub> and smoke. The drawback is that this reduction is often accompanied by an increase in emissions of CO and unburned hydrocarbons (UHC) [1].

Karim [2] described the dual fuel combustion process as proceeding in three stages after ignition in an indirect injection CI engine. The first stage is due to the combustion of approximately half of the pilot fuel and a small amount of gaseous fuel entrained within it. The second is due to diffusive combustion of the remaining pilot fuel and the rapid burning of gaseous fuel in the immediate surroundings. The third stage is due to flame propagation through the remainder of the cylinder charge. This description allows some explanation of dual fuel exhaust emission trends. For example, oxides of nitrogen (NO<sub>x</sub>) formation is known to be strongly dependent on local temperatures, so most NO<sub>x</sub> would be formed in the region around the pilot spray where high temperatures exist and the equivalence ratio is close to stoichiometric [3].

Dual fuel engines typically use either natural gas/methane or LPG/propane as the primary fuel [4]. The performance of different gaseous fuels as compared with each other is the subject of this present research, as they have not been directly compared in modern a DI diesel engine. For varying pilot quantity and gaseous fuel concentrations, three different fuels (methane, propane and butane) are compared as these factors have been identified as amongst the most important parameters influencing the dual fuel combustion process [5-7].

Methane, the main constituent of natural gas (typically 94% by volume in the UK), is a preferred fuel for use in dual fuel engines as it is highly knock resistant and contains more energy per unit mass than other conventional fuels, whilst fuel cost savings generally offset the cost of engine conversion [8]. It is the simplest and most stable hydrocarbon and its gaseous nature allows excellent mixing with air resulting in an even charge distribution and smoother heat release rates [1]. Methane has a wide flammability range, low global toxicity (as compared to diesel) and has low photochemical reactivity [9]. Most of the unburned hydrocarbon emissions from these engines are methane. Although it is chemically resistant and toxicologically inert, it has 12 to 30 times the greenhouse effect of carbon dioxide and so requires control [9].

Propane is the main constituent of LPG, and is attractive for use in dual fuel engines as it is a single, relatively simple species so engines and after treatment systems can be designed to utilize it cleanly [10]. It can be stored at atmospheric pressure so there are no evaporative losses. Propane has a good volumetric energy content and a road

octane number of more than 100. Consequently; it is considered that the most suitable use of LPG in engines is via dual fuel rather than bi fuel [11]. Although propane is normally regarded as a fast reacting fuel, it has an extended ignition delay period compared to methane [12, 13], and although it tends to produce slightly higher power due to the fast burning rates, it is ultimately possible to achieve higher power outputs with the more knock resistant methane.

Butane (a by-product of gasoline production) has a greater volumetric energy content than propane and it has a relatively low reactivity in the atmosphere [4]. Gota et al. [14] found that a butane/diesel dual fuel engine had a higher thermal efficiency than when fuelled with propane, and much reduced quantities of diesel were needed for ignition. Almost the same output was achieved with butane as with diesel alone over a wide load range, without smoke, and dual fuel operation was satisfactory at idle with 70% of the total heating value being supplied by butane. The butane/diesel engine had the same specific fuel consumption and reduced NO<sub>x</sub> emissions compared to diesel; however carbon monoxide levels were greatly increased. It was suggested that this effect was caused because butane acts as a reducing agent for NO<sub>x</sub>, but is itself oxidized to CO.

The primary gaseous fuels examined were chosen to represent compressed natural gas (CNG) and liquid petroleum gas (LPG). Propane and butane are both by-products of petroleum refining, and therefore are attractive alternative fuel supplies from an economic viewpoint.

## **2.0 EXPERIMENTAL PROCEDURE**

### **2.1 TEST FACILITY**

The present study focuses on the effect of concentration and type of gaseous fuel, and quantity of diesel pilot on engine performance of a dual fuel engine. In order to make direct comparisons between the various fuels and operating conditions, the operating conditions (e.g. injection timing) were not optimised. Details of the engine specification are given in Table 1.

The engine was coupled to a Heenan-Dynamatic MkII 220kW eddy current dynamometer which controlled and measured torque and speed, with a maximum error in speed of +/- 1 rpm and +/-2 Nm in torque. Intake airflow was measured using a laminar viscous flow air meter with a Type 5 Cussons manometer. Diesel fuel consumption was recorded using a volumetric fuel measurement system. The installation is shown schematically in Figure 1a.

High-speed data, comprising of cylinder pressure, fuel line pressure and crank angle were acquired using a National Instruments PCIO-MX16-E PC-BNC rack interface, coupled with a BNC 2090 capture board. Cylinder pressure was measured using a Kistler type 6053B60 piezocapacitive transducer connected to a Type 5011 charge amplifier. Dynamic fuel line pressure was obtained using a Kistler 4065A piezoresistive sensor and 4617A amplifier. This data was recorded with a resolution of 0.5 degrees crank angle on the falling edge of the signal from an AVL optical encoder, mounted directly on the engine crankshaft. The encoder also supplied a

single pulse per revolution signal to mark top dead centre and triggered data acquisition of 50 consecutive four stroke cycles for analysis.

## **2.2 DUAL FUEL CONVERSION**

Turner and Weaver [15] concluded that a simple central point mixing system is the most inexpensive and straight forward method of admitting a gaseous fuel to the dual fuel engine. To this end, a simple venturi type gas mixer valve was installed at a distance of ten pipe diameters upstream of the inlet manifold to ensure complete mixing of the air and fuel was achieved. Gaseous fuel flow rate was controlled by a needle valve located immediately upstream of an Omega FMA 1610 mass flow meter, which also recorded line pressure and fuel temperature. The details of this gas supply system are shown schematically in Figure 1b. The only other modification made to the engine was the replacement of the standard injectors with reduced flow injectors to improve injection performance.

## **2.3 METHOD**

Engine performance data were obtained under steady state operating conditions at three loads corresponding to  $\frac{1}{4}$ ,  $\frac{1}{2}$  and  $\frac{3}{4}$  load (relative to 100% load being 18.7kW), at an engine speed of 1500 rpm.

To ensure consistent operating conditions, the engine was run for approximately 10 minutes at 1500 rpm and  $\frac{1}{2}$  load until the cooling water temperature out of the cylinder head reached 80°C, and the exhaust gas temperature reached 250°C. The engine was then brought to the required test point, and allowed to settle before sampling of data began.

The first and last set of data to be acquired were for standard No. 2 diesel. The first data set served as a baseline to which subsequent results could be compared, and the last data set confirmed that the results were repeatable, and that the engine performance had not been impaired by the use of gaseous fuels. Selected key properties for the gaseous fuels are presented in Table 2.

### **3.0 HEAT RELEASE RATE ANALYSIS**

Heat release analysis of in-cylinder pressure data is a widely used combustion diagnostic tool, and reveals information regarding the rate processes and combustion characteristics occurring inside the engine. In itself, heat release rate is strongly related to emissions characteristics, which provides some information about the combustion process [16]. However; information about the time development of thermodynamic variables is also required.

The heat release analysis used here (based on [17]) consists of three control volumes, this is conceptually closer to dual fuel combustion where diesel is injected into an unburned zone, (air and a gaseous fuel) and eventually a burned zone is formed. This approach was also chosen because it allows a model for fuel injection to be derived from actual operating conditions. The assumptions made are;

- The combustion chamber consists of a diesel fuel zone, and unburned zone and a burned zone, (denoted by the subscripts f, u and b respectively). Each zone has uniform temperature, composition, and the pressure is uniform across the whole combustion chamber.
- The diesel fuel zone refers only to the diesel pilot which upon injection is assumed to instantly vaporise.



- The unburned zone into which fuel is injected is assumed to consist of air, exhaust gas residuals and gaseous fuel in their measured proportions.
- The burned zone appears when combustion begins, and is subsequently confirmed by finding the point at which the first derivative of pressure with respect to time reaches a minimum value [18].
- Combustion is assumed to occur due to the entrainment of the pilot fuel and unburned gasses and subsequent reactions in stoichiometric proportions.
- Individual species of the burned, unburned and vaporized fuel can be modelled as ideal gasses.

The total mass ( $m$ ) in the combustion chamber consists of the mass of the trapped air, ( $m_o$ ) which is air and residual exhaust gasses ( $m_a$ ), and in the dual fuel case, a gaseous fuel ( $m_g$ ). The charge air and gaseous fuel proportions are determined from measured mass flow rates, and the residual gas fraction is assigned an arbitrary value [17] (as the gas exchange process is not simulated). After the start of fuel injection, the mass of the cylinder also includes the mass of the fuel injected. Therefore the conservation of mass in the cylinder at any instant can be expressed as

$$m = m_u + m_b + m_f$$

where  $m = m_o + m_{fi}$  and  $m_o = m_a + m_g$  (1)

The rate at which the fuel zone and the unburned zones react to form the burned zone can be calculated by the difference between the mass of fuel injected at any instant ( $m_{fi}$ ) and the current mass in the fuel zone ( $m_f$ ) [17, 20]. For the dual fuel case there is the added complexity that the mass of the burned zone will also be a function of the

mass of gaseous fuel that has been burned during each time step. In order to express this, it is assumed that combustion occurs at a stoichiometric air fuel ratio ( $AFR_{S,tot}$ ) [3, 21, 22]. The  $AFR_{S,tot}$  has two hydrocarbon fuel components with molecular formulas of  $C_{xd}H_{yd}$  and  $C_{xg}H_{yg}$ ; and the mass ratio of the two fuels is also known [23]. Thus, the dual fuel  $AFR_{S,tot}$  is calculated as

$$\left(\frac{A}{F}\right)_{S,tot} = \frac{(\alpha(xd + yd/4) + \beta(xg + yg/4))MW_{air}}{\alpha(xdMW_C + ydMW_H) + \beta(xgMW_C + ygMW_H)} \quad (2)$$

Where

$$\alpha = \frac{m_d}{m_d + m_g} \text{ and } \beta = \frac{m_g}{m_d + m_g} \quad (3)$$

The mass of fuel burned is solved as part of the final equation set. If the overall dual fuel  $AFR_{S,tot}$  is maintained, then the mass of air entrained into the burned zone is given by:

$$m_b = (m_{fi} - m_f)(1 + AFR_{S,tot}) + (m_{fi} - m_f)\left(\frac{\beta}{\alpha}\right)(1 + AFR_{S,tot}) \quad (4)$$

Conservation of mass, ideal gas law and first law of thermodynamics [19] are applied to each zone so that at any instant, there are twelve unknowns to be solved; the three masses ( $m_u$ ,  $m_f$ ,  $m_b$ ), the three volumes ( $V_u$ ,  $V_f$ ,  $V_b$ ), the three temperatures ( $T_u$ ,  $T_f$ ,  $T_b$ ), and the three internal energies ( $u_u$ ,  $u_f$ ,  $u_b$ ). However, the system can be reduced to two ordinary differential equations and three algebraic equations.

$$\frac{dT_u}{d\theta} = \frac{dp}{d\theta} \frac{R_u T_u}{pc_{pu}} + \frac{dQ_u}{m_u c_{pu}} \quad (5)$$

$$\frac{dT_f}{d\theta} = \frac{dp}{d\theta} \frac{R_f T_f}{pc_{pf}} + \frac{\frac{dm_f}{d\theta} \left( \frac{1}{2} V_{inj}^2 \right) + \frac{dQ_f}{d\theta}}{m_f c_{pf}} \quad (6)$$

The unknowns are  $T_u$  and  $T_f$ , are solved by 4th Order Runge-Kutta method. Once  $T_u$  and  $T_f$  are known,  $m_u$ ,  $m_f$  and  $T_b$  are found from three algebraic equations that are solved by Newton–Rhapson technique [24]:

$$f_1(m_u, m_f, T_b) = m_u + m_f + (m_{fi} - m_f) (1 + AFR_{s,tot}) + (m_g - m_u \beta) (1 + AFR_{s,tot}) - m = 0 \quad (7)$$

$$f_2(m_u, m_f, T_b) = m_u R_u T_u + m_f R_f T_f \{ (m_{fi} - m_f) (1 + AFR_{s,tot}) + (m_g - m_u \beta) (1 + AFR_{s,tot}) \} R_b T_b - pV = 0 \quad (8)$$

$$f_3(m_u, m_f, T_b) = (m_u u_u + m_f u_f + R_b u_b \{ (m_{fi} - m_f) (1 + AFR_{s,tot}) + (m_g - \beta m_u) (1 + AFR_{s,tot}) \} - U_0 - Q_T - m_{fi} (h_f + \frac{1}{2} V_{inj}^2) + W = 0 \quad (9)$$

The main inputs to the model are a record of the cylinder pressure (p) against crank angle ( $\theta$ ), data for diesel fuel mass flow rate, needle lift, and fuel line pressure to determine the mass flow rate and injection velocity of the pilot fuel. Other inputs required are the inlet temperatures and mass flow rates of the gaseous fuel and air, from which initial conditions at inlet valve closure and the mass fractions of gaseous fuel and air can be calculated.

At start of injection the fuel zone comes into existence, and during the short ignition delay period, the values of temperature, heat transfer ( $dQ_u$  and  $dQ_f$ ) and internal energy are calculated. The burned zone then appears at the start of combustion, and equations (5) to (9) are solved. A record of the burned zone composition is preserved and used to calculate the new thermodynamic properties [25]. A schematic description of the three zone model is provided in Figure 2.

#### **4.0 Combustion Analysis Results**

Table 3 details the different fuelling conditions and Table 4 presents the key combustion phasing data. For this study, BSEC is employed due to the different calorific values of the fuels used.

##### **4.1 Brake Specific Energy Consumption**

Data are plotted to compare the three primary fuels in Figure 3 for the  $\frac{1}{4}$  load case at 1500 RPM (approx. 4.5 kW). As the equivalence ratio of each gaseous primary fuel is increased, BSEC increases slightly for the propane and butane cases. The greatest increase in BSEC was for the methane test results. It should be noted that a much greater volumetric quantity of methane was used to replace the diesel fuel than was possible to be achieved with propane (which exhibited knock at the highest levels) or butane (where the maximum fuel quantity was limited by the minimum pilot level that could be supplied). However; when the results are compared over the same fuelling range (up to  $\Phi(\text{primary})=0.10$ ) methane still shows the greater increase. If BSEC is to be taken as a measure of combustion completeness, then this would show that large amounts of unreacted methane are surviving through to the exhaust stage. On the basis of energy content, butane and propane are considered more reactive fuels than

methane and have reduced lower flammability limits (LFL % vol. Basis, [2]) and hence the combustion reactions of propane and butane are more complete at low loads and low equivalence ratios.

An anomalous result appears for methane at approximately  $\Phi(\text{primary}) = 0.17$ . This was caused by fluctuations in load and speed resulting in a disproportionately decreased diesel injection quantity (see Table 3). Consequently, this result should not be included in further analysis, but does show that BSEC increases with reduced pilot quantities.

The results were similar between  $\frac{1}{2}$  and  $\frac{3}{4}$  load, so the latter condition is presented in Figure 4. For methane, BSEC increased with increasing equivalence ratio; however, for propane and butane the BSEC decreased with increasing equivalence ratio. The most significant reduction being with propane. As load is increased, and hence so are cylinder temperatures, the combustion process becomes more complete and consumes more of the gaseous fuel. Maximum substitution levels were higher for propane than for butane, as the engine performance was limited by knock when fuelled with butane. This severe knocking caused the injector to fail at butane equivalence ratios greater than 0.2.

The methane BSEC increases at low equivalence ratios then decreases at high equivalence ratios. This was attributed to the fact that the methane equivalence ratio was too fuel lean to sustain a wide reaction zone around the ignition sites. Most of the energy contribution at these points is due to combustion of diesel fuel. As progressively more methane is added, a primary fuel equivalence ratio is reached

where methane can sustain a combustion reaction (coinciding with  $\Phi(\text{primary}) \approx 0.4$  in this data set). The reaction zone then becomes progressively wider and the overall combustion process becomes an increasingly strong function of the primary fuel concentration through a more significant diffusion burning period.

#### **4.2.1 Combustion Phasing Data Results**

The data within this section are presented in terms of rates of mass burnt; these results are directly proportional to those of heat release rate. The key results, with standard deviations, are presented in Table 4.

##### 4.2.1 Quarter Load Results

The data sets chosen for analysis were the lowest primary fuel substitution levels are presented in Figure 5.

As the primary fuel is increased, a greater degree of cyclic variability in the location of peak pressure was recorded. The most unstable and variable low load combustion process occurs when propane was used as the primary fuel, and an increasing variation in location of peak pressure is noted. The highest peak pressures are recorded with methane, as are the most stable combustion processes. Although ultimately higher equivalence ratios were obtained, less diesel energy was replaced by methane at the same equivalence ratio, and this larger pilot tends to promote a stable and positive combustion process. Propane and butane exhibit decreasing then

increasing peak cylinder pressures that occur later in the cycle. This indicates some change to the combustion process.

All three primary fuels showed reduced mass burning rates during premixed combustion and yielded higher diffusion burning rates compared with diesel. In other words, combustion of the gaseous fuel has begun to make a more significant contribution to the overall energy release rates. However; the combustion pattern remains similar in shape to that of diesel. Dual fuel combustion is known to be poor at light load, and this is shown by the reduced premixed combustion phase. Both propane and butane had higher diffusion combustion rates compared to methane (implying that they made a greater contribution to energy release). The diffusion burning rates of propane were the highest, although this is in part due to the later start of combustion for propane.

Injection timings were approximately the same for all data sets, but the addition of propane caused a more extended ignition delay than methane or butane. The addition of propane has a deleterious effect on pre-ignition processes leading to delayed start of combustion (SOC) and initially slower rates of mass burning, [13]. However; propane is considered to be a fast reacting fuel and in spite of the delayed SOC, mass burning rates subsequently exceed those of butane, but do not quite catch up with methane. It can be concluded that at low load, a more reactive primary fuel will result in a delayed combustion process through its competition for pre-ignition reaction radicals.

Butane's competition with the diesel pilot for active radicals [13] leads to reduced (but not delayed) initial mass burning rates and a less positive, less rapid and less

wide reaching ignition process. At the same time, butane requires a greater quantity of oxygen than propane for complete combustion. Therefore, local conditions in the reaction zone were fuel rich, and overall the combustion process was less complete.

### 5.2.1 Half Load Results

The lowest primary fuel substitution levels at  $\frac{1}{2}$  load are shown in Figure 6. Although the propane equivalence ratio is slightly lower, injection timings are similar for all three fuels. Methane has a slightly reduced mass burning rates during the premixed phase of combustion and almost identical rates of diffusion burning relative to diesel. Propane has slightly higher rates during both phases compared with the methane case. The differences for butane are more pronounced, and although SOC was slightly advanced compared with methane and propane, the premixed peak is much lower. This is further evidence of butane competing with and impeding the combustion process of the diesel pilot as mass burning rates throughout premixed combustion were reduced. The distinction between premixed and diffusion burning phases is also less pronounced due to a less positive ignition source provided by the pilot, and a widened reaction zone around each ignition point.

Figure 6 also shows that for all three fuels the combustion process is strongly dependent on the pilot, and that when the pilot has been consumed, combustion ends.

The maximum primary fuel substitution levels are compared in Figure 7. The maximum methane equivalence ratio was significantly higher than for propane or butane and so a similar methane fuelling level ( $\Phi \approx 0.18$ ) is also compared. A



different combustion pattern emerges for butane than has been seen previously, and is evidence of a fuel rich, fast, combustion process that can occur at mid point substitution levels. The initial mass burning rates and premixed peak of butane are lower than for propane and methane, however the diffusion burning rates are greatly elevated. Combustion duration is reduced for butane, and the sharp decrease in the rate of mass burning at the end of the combustion period would suggest that, again, when the pilot is consumed, the combustion process ends.

### 5.2.2 Three Quarters Load Results

In Figure 8, the lowest gaseous fuel substitution cases are compared, and the overall shape of the combustion process is similar that of diesel combustion. This suggests that the combustion processes at this load are a strong function of the pilot reactions, and because the combustion pattern hasn't changed significantly from that recorded at lower loads, the increased combustion temperatures are less important than fuelling levels. Ignition timing, for these cases, was held constant between the three fuels which allows for a clearer comparison of the trends. Propane again shows lower initial mass burning rates, but in the higher cylinder temperatures at  $\frac{3}{4}$  load, this effect is reduced and the mass burning rate ultimately exceeds methane and butane. The initial mass burning rates are highest for butane, but the continued competition between butane and diesel, for oxygen, ultimately result in a lower premixed peak. This supports the argument that there continues to be a diesel combustion reaction throughout the combustion process. The diffusion burning rates for butane are higher, supporting the argument that butane results in the widest reaction zone surrounding ignition sites.

The maximum substitution levels at  $\frac{3}{4}$  load are shown in Figure 9. The maximum propane fuelling level was limited by knock, and butane data set was limited by the failure of the injector tip. All three fuels show a greatly increased contribution to energy release during the diffusion burning period. As it was possible to achieve significantly higher methane equivalence ratios, the mass burning rates continue to increase during the diffusion period. The small diesel pilot ignites and in doing so the methane in the surrounding reaction zone also ignites. The high methane equivalence ratio allows the burning methane to ignite portions of methane/air mixture that are not in direct contact with the diesel pilot ignition sites and more of a flame propagation process occurs. However; there is a definite premixed and diffusion burning phase which would imply that flame propagation is not independent of the pilot.

## **6.0 CONCLUDING SUMMARY**

This paper has investigated three alternative fuels, based upon CNG and LPG, for use in a dual fuel engine and has reported the effects of the fuel and concentration on BSEC and combustion phasing.

The three zone model has identified that three different combustion patterns occur as the concentration of gaseous fuel is increased. At low primary fuel substitution levels, the combustion pattern closely follows diesel. At high substitution levels the classic dual fuel combustion process as described by Karim [2] is observed, but between the two patterns there is a transition region. The change from one regime to

another occurs earlier when the gaseous fuel is more reactive, and is a stronger function of fuelling strategy than cylinder temperature. The behavior during this period is also a function of the primary fuel. Propane had the longest ignition delays due its competition with diesel for pre-ignition reaction radicals. However, the mass burned rates quickly increase during the premixed phase and exceed those of methane and butane. This is attributed to the fast reactions of propane that are readily able to ignite portions of the propane air mixture that are not in direct contact with the pilot.

Butane suffers from a continued competition between the pilot and primary fuel that tends to slow down mass burned rates throughout the premixed phased. Diffusion rates are elevated compared with methane and propane only when a limiting concentration of butane has been reached.

Finally, methane shows a much stronger dependence on the pilot than either propane or butane and so this mechanism where burning methane ignites portions of methane only occurs at the very highest concentrations.

## **7.0 REFERENCES**

1. **Karim, G.A.**, The Dual Fuel Engine of the Compression Ignition Type - Prospects, Problems and Solutions - A Review, *SAE Paper Number 831073*, 1983
2. **Karim, G.A.**, Combustion in Gas Fuelled Compression-Ignition Engines, *ASME ICE Fall Technical Conference*, 2000, **351**
3. **Kishnan, S.R., M. Biruduganti, Y. Mo, S.R. Bell, and K.C. Midkiff**, Performance and Heat Release Analysis of a Pilot-Ignited Natural Gas Engine, *IMechE*, 2002,.

4. **Patil, P.G.**, Alternative Fuels in Future Vehicles, *Automotive Engineering*, 1996, **1041**
5. **Gebert, K., Beck, N.J., Barkhimer, R.L., and Wong, H.C.** Strategies to Improve Combustion and Emission Characteristics of Dual-Fuel Pilot Ignited Natural Gas Engines, *SAE Paper Number 971712*, 1997
6. **Lin, Z., and Su, W.** A Study on the Determination of the Amount of Pilot Injection and Rich and Lean Boundaries of the Pre-Mixed CNG/Air Mixture for CNG/Diesel Dual-Fuel Engine, *SAE Paper Number 2003-01-0765*, 2003
7. **Mbarawa, M., Milton, B.E., and Casey, R.T.** An investigation of the effects of diesel pilot injection parameters on natural gas combustion under diesel conditions, *Journal of the Institute of Energy* 2001, **74**
8. **Park, T., Atkinson, R.J., Clark, N.N., Traver, M.L., and Atkinson, C.M.**, Operation of a Compression Ignition Engine with a HEUI Injection System on Natural Gas with Diesel Pilot Injection, *SAE Paper Number 1999-01-3522*, 1999
9. **Liu, B., Checkel, M.D., Hayes, R.E., Zheng, M. and Mirosh, E.**, Experimental and Modelling Study of Variable Cycle Time for a Reversing Flow Catalytic Converter for Natural Gas/Diesel Dual Fuel Engines, *SAE Paper Number 2000-01-021*, 2000
10. **Newkirk, M.S., Smith, L.R., Payne, M.L., and Seagal, J.S.**, Emissions with butane/propane blends, *Automotive Engineering*, 1996, **104** (11)
11. **Pirouzpanah, V. and Nohammadi, A.B.**, Dual-Fuelling of an Industrial Indirect Injection Diesel Engine by Diesel and Liquid Petroleum Gas, *International Journal of Energy Research*, 1996, **20**
12. **Karim, G.A. and Rogers, A.**, Comparative studies of propane and butane as dual-fuel engine fuels, *Journal of the Institute of Fuel*, 1967, **40** (322)

13. **Liu, Z. and Karim, G.A.**, The Ignition Delay Period in Dual Fuel Engines, *SAE Paper Number 950466*, 1995
14. **Goto, S., Furutani, H., Komori, M., and Yagi, M.**, LPG-Diesel Engine, *International Journal of Vehicle Design*, 1994, **153**(4/5)
15. **Turner, S.H. and Weaver, C.S.**, Dual-Fuel Natural Gas/Diesel Engines: Technology, Performance, and Emissions, *Gas Research Institute*, 1994, **Report Number GRI-94/0094**
16. **Bruntt, M.F.J. and Platts, K.C.**, Calculation of Heat Release in Direct Injection Diesel Engines, *SAE Paper Number 1999-01-0187*, 1999
17. **Sastry, G.V.J. and Chandra, H.**, A Three-Zone Heat Release Model for DI Diesel Engines, *SAE Paper Number 94067*, 1994
18. **Stone, R.**, Introduction to Internal Combustion Engines, *Macmillan Press Ltd.*, 1999
19. **Heywood, J.B.**, Internal Combustion Engine Fundamentals, *McGraw-Hill*, 1988
20. **Timoney, D.J., McNally, C.P., and Doyle, C.T.**, A Three-Zone Heat Release Model for Direct Injection Diesel Engines, *Theisel*, 2000
21. **Khan, M.O.**, Dual-Fuel Combustion Phenomena, in Department of Mechanical Engineering. *Phd Thesis*, 1969, Imperial College of Science and Technology: London. p. 289.
22. **Pirouzpanah, V. and Amiraslani, K.**, A model to predict performance and heat release of dual-fuel diesel engines, in *Symposium on Gas Engines and Co-Generation*, 1990, Solihull: MEP.
23. **Liu, Z. and Karim, G.A.**, Simulation of combustion processes in gas-fuelled diesel engines, *Proceedings of the Institute of Mechanical Engineers*, 1997 **211**(A)

24. **Press, W.H., Teukolsky, S.A., Vetterling, W.T., and Flannery, B.P.** Numerical Recipes in Fortran 77: The Art of Scientific Computing, *Cambridge University Press*, 1992
25. **Olikara, C. and Borman, G.L.** A Computer Program for Calculating Properties of Equilibrium Combustion with Some Applications to I.C. Engines, *SAE Paper Number 750468*, 1975
26. **Karim, G.A., Liu, Z. and Jones, W.** Exhaust Emissions from Dual Fuel Engines at Light Load, *SAE Paper Number 932822*, 1993
27. **Poonia, M.P., Ramesh, A., and Gaur, R.R.,** Effect of Intake Temperature and Pilot Fuel Quantity on the Engine Combustion Characteristics of a LPG Diesel Dual Fuel Engine, *SAE Paper Number 982455*, 1998
28. **Karim, G.A., Liu, Z. and Jones, W.** Exhaust Emissions from Dual Fuel Engines at Light Load, *SAE Paper Number 932822*, 1993
29. **Karim, G.A., Jones, W. and Raine, R.R.** An Examination of the Ignition Delay Period in Dual Fuel Engines, *SAE Paper Number 892140*, 1989
30. **Patterson, J., Clarke, A., and Chen, R.** Experimental Study of the Performance and Emissions Characteristics of a Small Diesel Genset Operating in Dual-Fuel Mode with Three Different Primary Fuels, *SAE Paper Number 2006-01-0050*, 2006

## **List of Tables**

Table 1 – Engine Specifications

Table 2 – Selected Properties of the gaseous fuels, Properties of diesel from ESSO Ultra Low Sulphur Diesel from Esso Marketing Technical Bulletin (ExxonMobil, 2001), Properties of gaseous fuels from manufacturers data sheets

Table 3 - Comparison of Fuelling Conditions

Table 4 - Comparison of Combustion Phasing Parameters

## **List of Figures**

Figure 1 - Schematic diagram of the test engine and dual fuel conversion

Figure 2 – Schematic description of the three zone model

Figure 3 – Comparison of BSEC at  $\frac{1}{4}$  load and 1500 rpm

Figure 4 – Comparison of BSEC at  $\frac{3}{4}$  load and 1500 rpm

Figure 5 – Comparison of minimum and same equivalence ratios at  $\frac{1}{4}$  load

Figure 6 – Comparisons of minimum primary substitution at  $\frac{1}{2}$  load

Figure 7 – Comparisons of maximum and same primary equivalence ratio at  $\frac{1}{2}$  load

Figure 8 – Comparisons of minimum primary substitution at  $\frac{3}{4}$  load

Figure 9 – Comparison of maximum and same primary equivalence level at  $\frac{3}{4}$  load

Engine Type	Lister-Petter 4x90, DI, 4stroke, naturally aspirated diesel
Configuration	Vertical in-line 4 cylinder
Cylinder Bore x Stroke	90 x 90 mm
Connecting Rod Length	138 mm
Compression Ratio	18.5:1
Total displacement	2.29 litres
Rated Speed	1800 rpm
Rated Power	37.5 kW at 2100 rpm
Fuel Injection Pump	Lucas Rotary

Table 1 – Engine Specifications

Fuels	Methane	Propane	Butane	Diesel
Chemical Formula	CH <sub>4</sub>	C <sub>3</sub> H <sub>8</sub>	C <sub>4</sub> H <sub>10</sub>	~ C <sub>12</sub> H <sub>26</sub>
Molecular Weight	16	44	58	~170
Density at STP (kg/m <sup>3</sup> )	0.647	1.779	2.345	~840
LHV (MJ/kg)	50.05	46.33	45.73	42.9
Stoichiometric Air/Fuel	17.2	15.7	15.5	14.5
Cetane Number	~ 0	~ 0	~ 5	40-55
Flammability U	15.0	9.5	8.5	7.5
Limits L (% by volume of gas in air)	5.0	2.2	1.5	0.6

Table 2 – Selected Properties of the gaseous fuels, Properties of diesel from ESSO Ultra Low Sulphur Diesel from Esso Marketing Technical Bulletin (ExxonMobil, 2001), Properties of gaseous fuels from manufacturers data sheets



Primary (Φ)	% Energy supplied by primary	% Energy supplied by pilot
<b>Methane ¼ Load</b>		
0.02	9.76	90.24
0.12	43.98	56.02
0.29	65.42	34.58
<b>Propane ¼ Load</b>		
0.01	6.36	93.64
0.03	16.31	83.69
0.11	49.84	50.16
<b>Butane ¼ Load</b>		
0.02	10.30	89.70
0.03	15.93	84.07
0.11	42.92	57.08
<b>Methane ½ Load</b>		
0.03	9.68	90.32
0.18	45.86	54.14
0.33	71.06	28.94
<b>Propane ½ Load</b>		
0.01	3.99	96.01
0.16	58.83	41.17
<b>Butane ½ Load</b>		
0.03	9.72	90.28
0.16	43.91	56.09
<b>Methane ¾ Load</b>		
0.05	10.47	89.53
0.13	26.08	73.92
0.70	82.01	17.99
<b>Propane ¾ Load</b>		
0.03	6.42	93.58
0.15	40.83	59.17
0.23	66.84	59.17
<b>Butane ¾ Load</b>		
0.05	10.82	89.18
0.12	26.47	73.53
0.20	43.47	56.53

Table 3 – Comparison of Fuelling Conditions

Primary (Φ)	Pmax (bar)	Location	Sdev P	Sdev (CA)	SOC (CA degrees)	Duration (CA)	SOI (CA degrees)	Ignition Delay
<b>Methane ¼ Load</b>								
0.02	49.98	4.00	0.47	0.35	-4.5	28.5	-11.5	7.0
0.12	46.99	4.50	0.64	0.31	-3.0	28.5	-10.0	7.0
0.29	47.35	5.00	0.51	0.61	-3.5	30.5	-11.5	7.5
<b>Propane ¼ Load</b>								
0.01	49.732	4.0	0.406	0.524	-4.0	28.0	-11.0	7.0
0.03	44.614	4.5	0.685	0.438	-2.5	27.5	-9.5	7.0
0.11	45.849	5.5	1.078	0.612	-1.5	29.5	-9.5	8.0
<b>Butane ¼ Load</b>								
0.02	44.932	4.5	0.823	0.521	-3.0	29.5	-9.5	6.5
0.03	44.997	4.5	0.866	0.44	-3.0	28.5	-9.5	6.5
0.11	46.224	5.0	0.572	0.679	-3.0	29.0	-9.5	6.5
<b>Methane ½ Load</b>								
0.03	49.40	0.50	0.43	0.27	-1.5	30.5	-8.0	6.5
0.18	52.76	5.00	0.59	0.52	-4.0	30.5	-11.5	7.5
0.33	51.40	7.00	1.33	0.55	-3.0	32.0	-10.5	7.5
<b>Propane ½ Load</b>								
0.01	50.42	7.0	0.502	0.468	-1.5	30.0	-8.0	6.5
0.16	47.308	7.0	1.668	0.657	-1.5	31.0	-9.5	8.0
<b>Butane ½ Load</b>								
0.03	49.11	7.0	0.672	0.497	-2.0	29.5	-8.5	6.5
0.16	54.545	9.5	1.224	0.54	-3.0	28.5	-9.0	7.0
<b>Methane ¾ Load</b>								
0.05	49.63	8.00	0.47	0.38	-0.5	31.0	-6.5	6.0
0.13	51.10	8.00	0.52	0.36	-1.0	32.0	-7.5	6.5
0.70	50.32	11.50	1.24	0.93	-1.5	32.0	-7.5	6.0
<b>Propane ¾ Load</b>								
0.03	50.48	8.5	0.414	0.482	-0.5	31.0	-6.5	6.0
0.15	51.632	12.0	3.989	1.513	-3.5	28.0	-11.0	7.5
0.23	52.481	8.0	0.562	0.542	-1.0	30.0	-8.0	7.0
<b>Butane ¾ Load</b>								
0.05	48.896	9.0	0.505	0.619	-1.0	31.0	-6.5	5.5
0.12	51.606	9.5	0.742	0.511	-2.0	32.5	-7.5	5.5
0.20	57.73	8.5	0.92	0.46	-3.5	31.5	-9.0	5.5

Table 4 - Comparison of Combustion Phasing Parameters

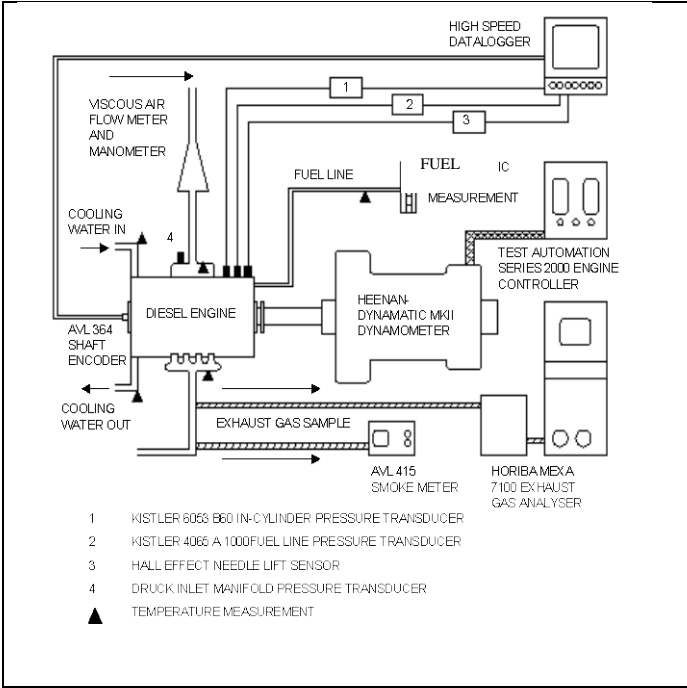


Figure 1a

Schematic diagram of the engine and equipment

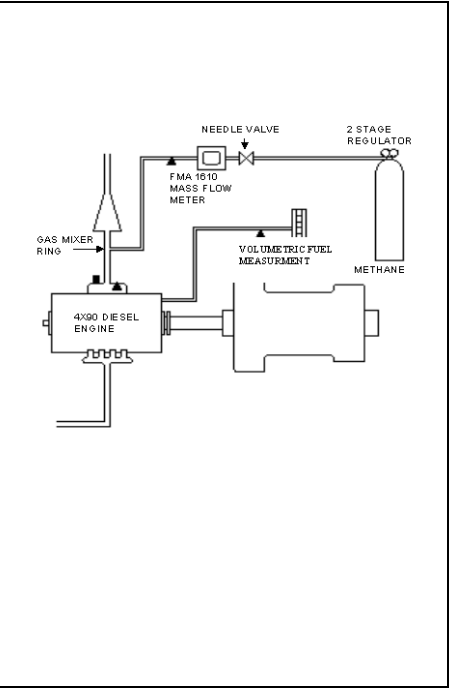


Figure 1b

Schematic of gas installation

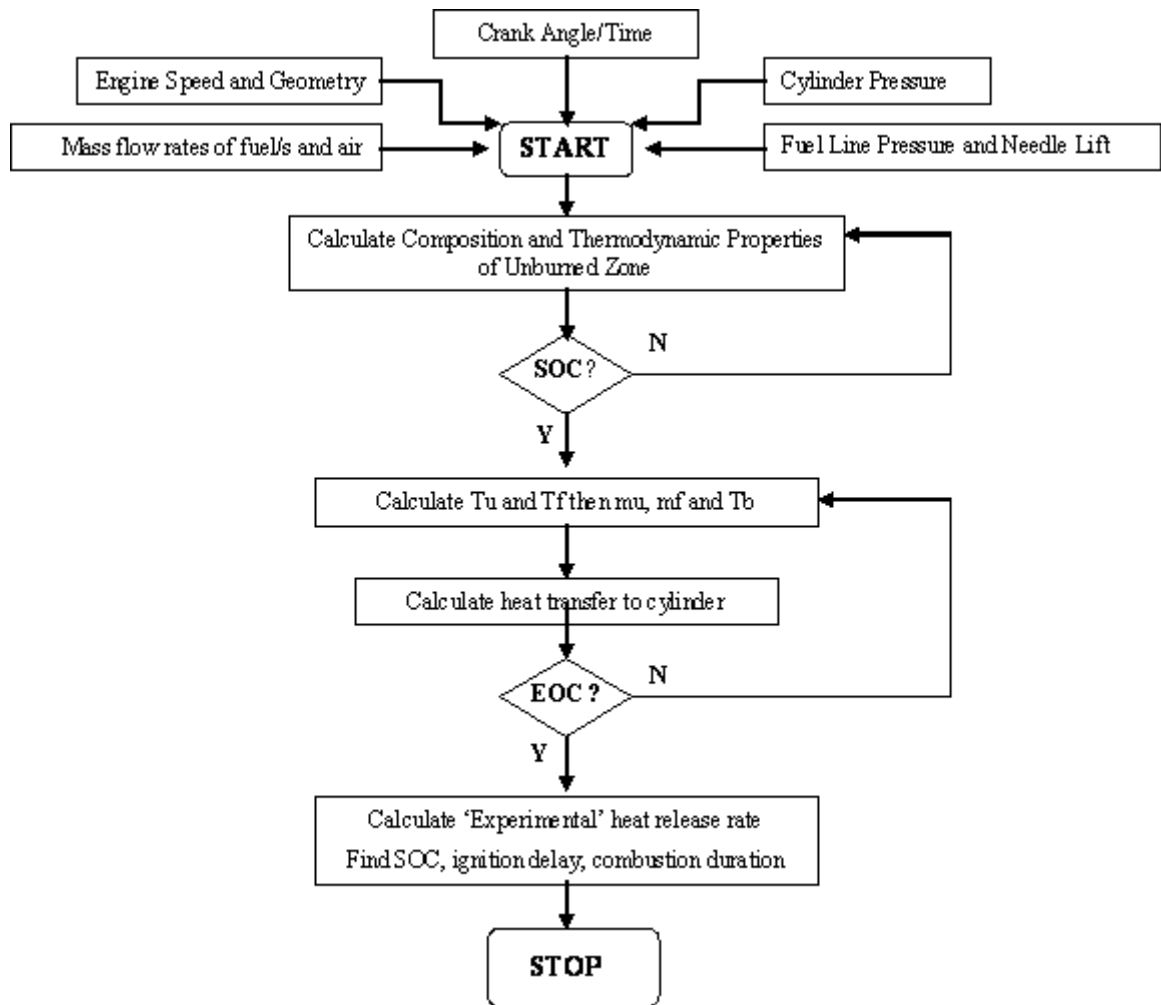


Figure 2 – Schematic description of three zone model.

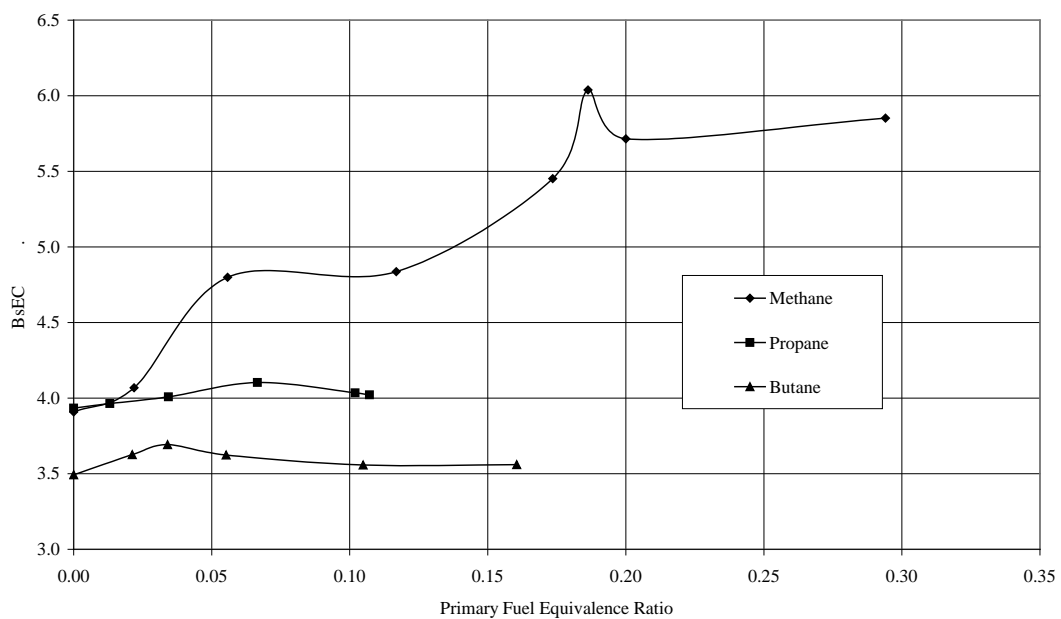


Figure 3 – Comparison of BsEC at 1/4 load and 1500 rpm.

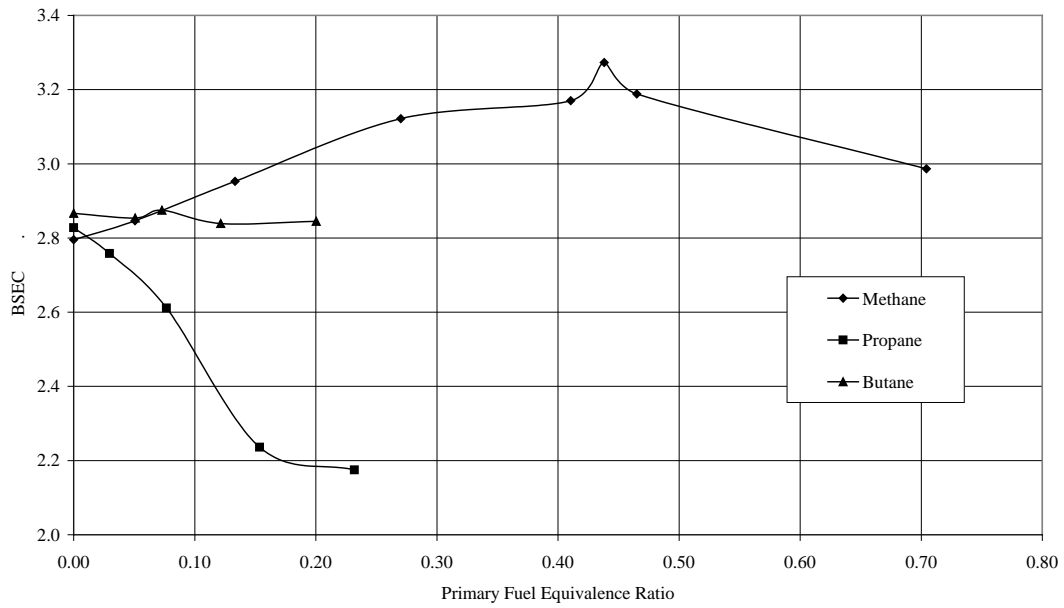


Figure 4 – Comparison of BSEC at  $\frac{3}{4}$  load and 1500 rpm.

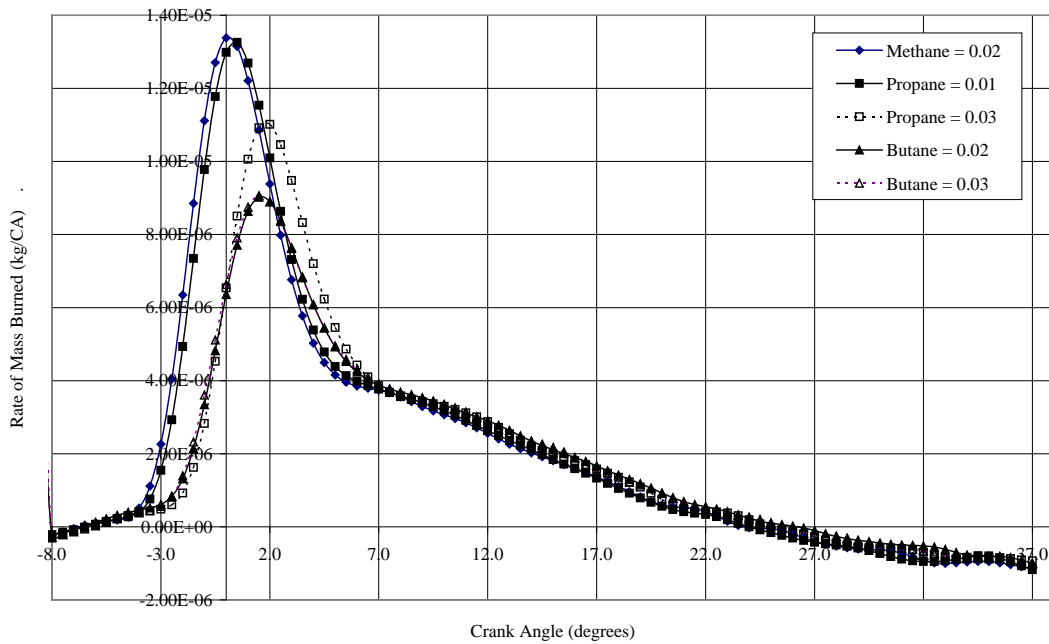


Figure 5 – Comparison of minimum and same equivalence ratios at  $\frac{1}{4}$  load.

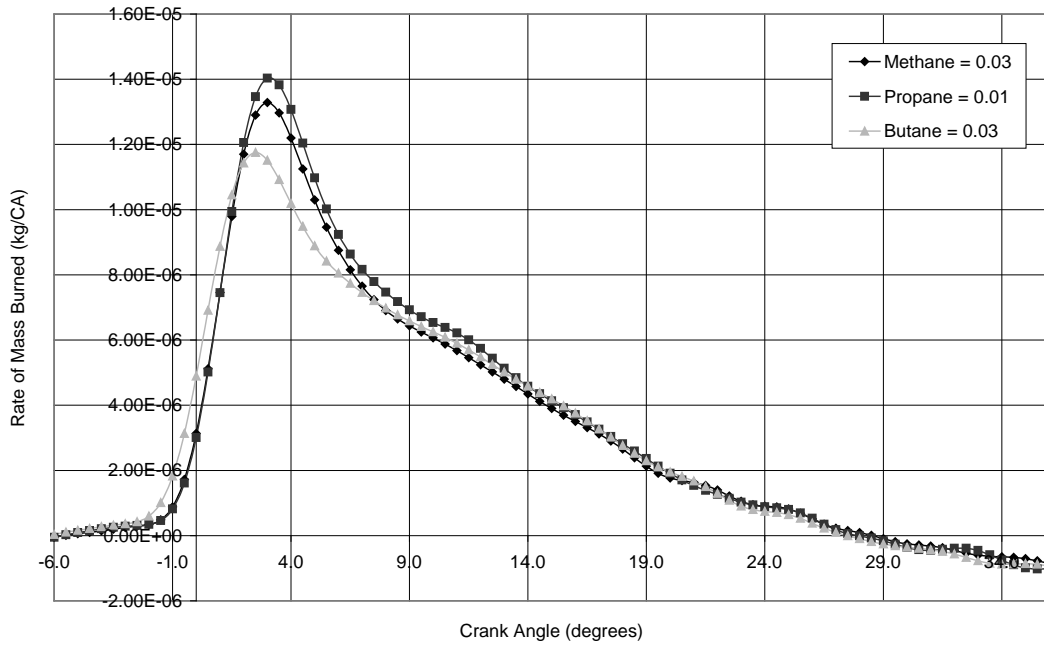


Figure 6 – Comparisons of minimum primary substitution at 1/2 load

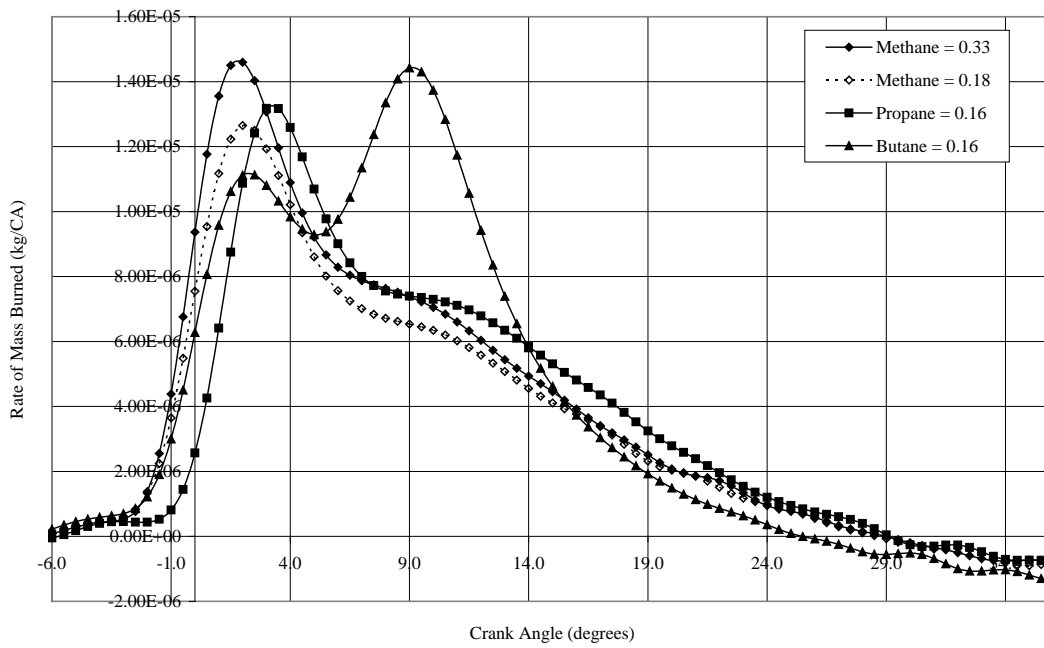


Figure 7 – Comparisons of maximum and same primary equivalence ratio at 1/2 load

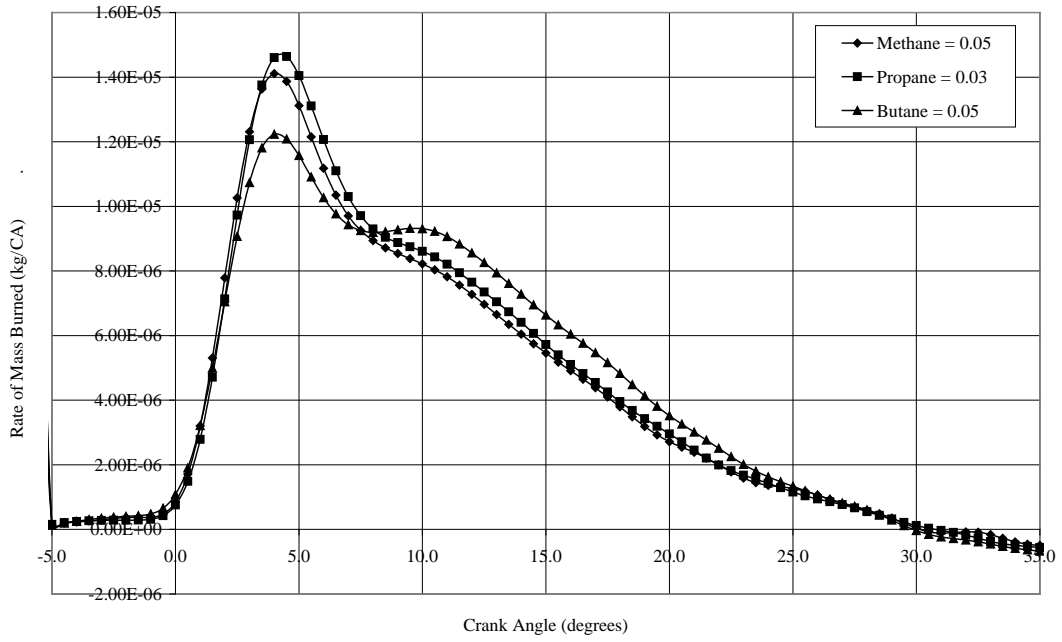


Figure 8 – Comparisons of minimum primary substitution at  $\frac{3}{4}$  load

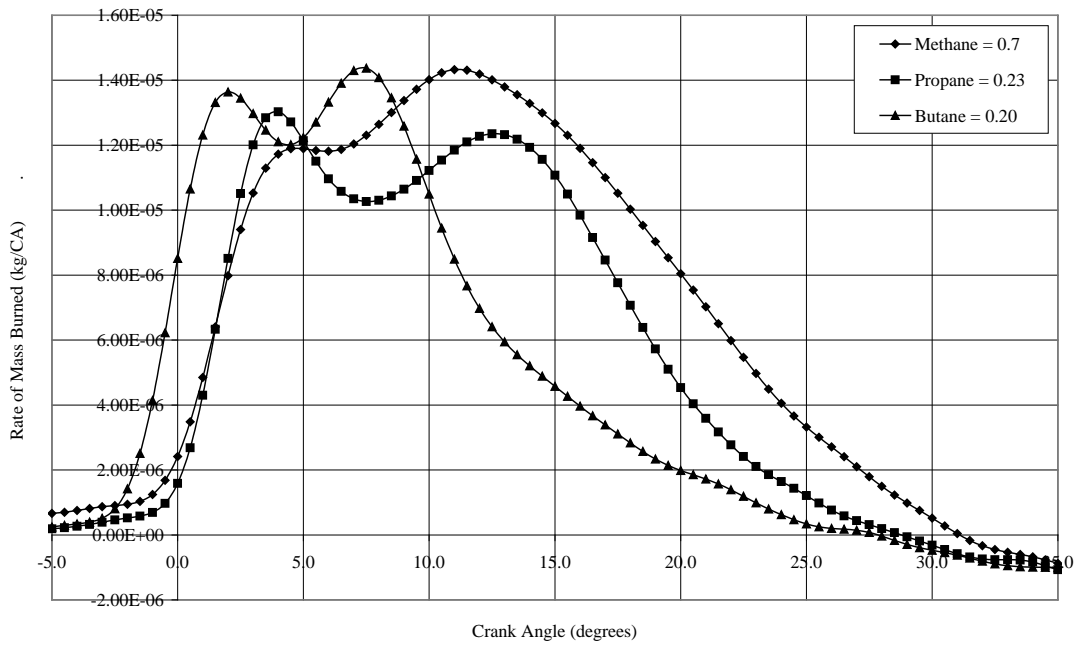


Figure 9 – Comparison of maximum and same primary equivalence level at  $\frac{3}{4}$  load